Zoologischer Anzeiger 267 (2017) 101–110

Contents lists available at ScienceDirect

Zoologischer Anzeiger

journal homepage: www.elsevier.com/locate/jcz

Zoologischer Anzeiger

Delayed osteogenesis and calcification in a large true toad with a comparative survey of the timing of skeletal ossification in anurans

Raúl O. Gómez[a,c,*], Eleonora Regueira[b,c], M.E. Ailín O'Donohoe[b,c], Gladys N. Hermida[b,**]

[a] Universidad de Buenos Aires, Facultad de Ciencias Exactas y Naturales, IGEBA-CONICET, Ciudad Universitaria, C1428EGA Buenos Aires, Argentina
[b] Universidad de Buenos Aires, Facultad de Ciencias Exactas y Naturales, Departamento de Biodiversidad y Biología Experimental, Ciudad Universitaria, C1428EGA Buenos Aires, Argentina
[c] Consejo Nacional de Investigaciones Científicas y Técnicas (CONICET), Buenos Aires, Argentina

ARTICLE INFO

Article history:
Received 23 December 2016
Received in revised form 3 March 2017
Accepted 3 March 2017

Keywords:
Anura
Bufonidae
Rhinella arenarum
Skeletogenesis
Ossification sequence
Histology

ABSTRACT

Postembryonic skeletogenesis in anuran amphibians has been widely studied, yet less than one percent of the extant diversity has been covered and relatively few comparative studies exist. Here we document the sequence and timing of ossification of the Common Toad *Rhinella arenarum*, a large true toad (Bufonidae) from South America that is a model organism for varied ongoing research. We study histological sections and cleared-and-stained specimens of an ontogenetic series ranging from early larval stages to juveniles, documenting the ossification sequence of the entire skeleton. To diminish potential environmental biases we also study the skeletogenesis of the frog *Leptodactylus latinasus* (Leptodactylidae) from the same pond and season. We summarize comparative data from numerous anuran species to contextualize our results in a broad phylogenetic context. Histological data shows that skeletal calcification in *R. arenarum* is temporally dissociated from osteoid matrix formation and occurs later than in most other anurans, which is unexpected given its generalized pond-type larva and heavily ossified adult skeleton. At the onset of metamorphosis, exoccipitals, parasphenoid, and frontoparietals are the only ossified skull elements, whereas most of the postcranium has already started ossification. This pattern is rare among anurans but is shared by other bufonids, in which it has been previously linked to rapid development. Our comparative survey, however, suggests that the delayed bufonid pattern is not related to fast-developing larvae but instead might be a distinctive feature of true toads.

1. Introduction

Postembryonic skeletogenesis in anuran amphibians has been intensively studied, with many previous work focusing on osteological descriptions and ossification sequences of particular species (e.g., Haas, 1999; Hall and Larsen, 1998; Maglia, 2003; Maglia and Pugener, 1998; Shearman and Maglia, 2015; Trueb and Hanken, 1992; Vera and Ponssa, 2014; Wild, 1997; Yıldırım and Kaya, 2014). However, less than one percent of the extant anuran species have been analyzed so far and this type of information has seldom been summarized by comparative studies (e.g., Harrington et al., 2013; Trueb, 1985; Weisbecker and Mitgutsch, 2010), and most of the latter have focused on the skull. Although a fairly conserved developmental pattern exists, there is considerable variation among anurans in the sequence of appearance of particular bones, timing of ossification relative to external morphology, and larval period length (Fabrezi, 2011; Harrington et al., 2013). Interestingly, bones that appear late in the ossification sequence of many anurans convergently fail to ossify in other lineages, which points to a link between timing of osteogenesis and ossification (Trueb and Alberch, 1985; Weisbecker and Mitgutsch, 2010).

Bone formation in the anuran larvae has been described to proceed by formation of osteoid matrix first, with subsequent calcification at later stages (Hanken and Hall, 1988), although this has been documented in a single species to date. In addition, not all the skeleton necessarily ossifies at the same moment, with an important decoupling between cranial and post-cranial ossification having been previously documented (e.g., Dunlap and Sanchiz, 1996). Particularly, Dunlap and Sanchiz (1996) found a delayed pattern of cranial ossification relative to the appendicular skeleton in two bufonid species that they related to a rapid larval develop-

* Corresponding author at: Universidad de Buenos Aires, Facultad de Ciencias Exactas y Naturales, IGEBA-CONICET, Ciudad Universitaria, C1428EGA Buenos Aires, Argentina.
** Corresponding author.
E-mail addresses: raulgomez@gl.fcen.uba.ar (R.O. Gómez), gladyshermida@gmail.com (G.N. Hermida).

http://dx.doi.org/10.1016/j.jcz.2017.03.002
0044-5231/

ment; a hypothesis that remains to be tested. It should be noted, however, that the larval period lengths of these true toads are not especially short, as shown by the comparative data now available (e.g., Fabrezi, 2011).

The Common Toad *Rhinella arenarum* (Hensel, 1867) (Bufonidae) is a large true toad (88–112 mm; Cei, 1980) from southern South America with a generalized pond-type larva (Altig and Johnston, 1989; Vera Candioti, 2006) and a heavily ossified adult skeleton (Pérez Ben et al., 2014). Together with nearly a hundred species in the same genus, it is part of a widely distributed neotropical radiation that includes most of the former South American *Bufo* Garsault, 1764 (Frost, 2016). This large toad is a common species across most of its wide range and it is a model organism, either at embryonic, larval or adult stages, for ongoing research on histology, endocrinology, ecotoxicology, and cognition, among other topics (e.g., Attademo et al., 2017; Hermida and Farías, 2009; Pollo et al., 2015; Regueira et al., 2013a,b, 2016, 2017; Sotelo et al., 2015). Despite this, there is a remarkable lack of information about its skeletogenesis.

Here we study the sequence and timing of ossification of the entire skeleton of *R. arenarum* through examination of histological sections and cleared-and-stained specimens of an ontogenetic series ranging from early larval stages to juveniles, taking into account intraspecific variation. We aim to explore if osteoid matrix formation and bone matrix calcification are temporally decoupled and to examine the patterns of cranial relative to the appendicular ossification in this species. Finally, we summarize comparative data of a diverse sample of anurans in order to test previous hypotheses regarding the link between delayed cranial ossification and larval period length and to contextualize our observations in a broad phylogenetic context.

2. Materials and methods

2.1. Animals

An ontogenetic series of larvae and juveniles of *R. arenarum* was obtained mostly from wild-caught specimens from temporary ponds at Ciudad Universitaria, Buenos Aires, Argentina. To complete this series, tadpoles were reared at the laboratory in dechlorinated tap water under a natural photoperiod and temperature and fed *ad libitum* with boiled chard. The larvae were staged according to the developmental scheme of Gosner (1960) and the postembryonic larval period was divided into premetamorphosis, prometamorphosis, and metamorphosis (= metamorphic climax) following Etkin (1932). After metamorphosis, newly metamorphosed toadlets were reared under natural outdoor conditions for 6–10 days. Additionally, we studied larvae of *Leptodactylus latinasus* Jiménez de la Espada, 1875, which skeletal ossification have previously been studied (Fabrezi, 2011; Supplementary data), that were collected from the same pond as some of the larvae of *R. arenarum* and reared in the same conditions, in order to lessen potential environmental biases on the timing of ossification. The rationale behind this comparison is that, if a pervasive environmental effect on the ossification is present, whatever it is, it would equally affect both species.

Animals were euthanized by immersion in 0.1% aqueous solution of MS222 (tricaine methanesulfonate; Sigma-Aldrich, St. Louis, MI). The ontogenetic series of *R. arenarum* consists of a total of 130 specimens, including tadpoles of every Gosner stage (hereafter GS) ranging from GS25 to GS45, newly metamorphosed toadlets (GS46), and juveniles (J), whereas the series of *L. latinasus* include 26 specimens representing all stages from GS33 to GS46 (Supplementary data). All the specimens were deposited at the herpetological collection of Laboratorio de Biología de Anfibios, Facultad de Ciencias Exactas y Naturales, Universidad de Buenos Aires, Argentina. This study was carried out in accordance with the regulations specified by the Institutional Animal Care and Use Committee of the Facultad de Ciencias Exactas y Naturales, Universidad de Buenos Aires (Res C/D 140/00) and the National Institutes of Health guide for the care and use of Laboratory animals (NIH Publications No. 8023, revised 1978). The Conservation category of *R. arenarum* and *L. latinasus* is "Least concerned" according to the IUCN Red List criteria (IUCN, 2016) and Vaira et al. (2012).

2.2. Histological and histochemical techniques

Three to seven specimens per stage of *R. arenarum* (99 specimens in total) and one to three specimens per stage of *L. latinasus* (26 specimens in total) were fixed and stored in 10% buffered formaldehyde and cleared and double-stained for bone (Alizarin Red) and cartilage (Alcian Blue) following Wassersug (1976). Specimens were examined under a Zeiss Stemi SV-11 stereomicroscope and photographed using a Nikon D3200 digital camera equipped with a macro lens.

For histological serial sections of *R. arenarum*, 31 animals of selected stages (GS27–46; Supplementary data) were fixed in Bouin's solution for 24 h, embedded in paraffin, and then sectioned in a transverse or sagittal plane at 6 μm (Kiernan, 1999). Sections were stained with modified Masson's trichrome (MMT) stain for general cytology and histology (Regueira et al., 2016). MMT is different from the original Masson's trichrome in that the acid fuchsin solution (0.03% p/v) also contains orange G (0.07% p/v) and xylidine ponceau (0.07% p/v). MMT stained osteoid matrix vividly blue, due to aniline blue affinity for collagen fibers. In addition, von Kossa method was performed to clearly detect calcified matrix (brown; Kiernan, 1999). Histological sections were studied and photographed using a Zeiss Primo Star microscope with an attached Canon PowerShot A640 digital camera.

2.3. Ossification data, criteria and indexes

We accounted for the sequence (i.e., relative order of appearance) of 18 cranial, three axial, and 16 appendicular bones, as well as for their timing of ossification according to Gosner stage, based on examination of cleared-and-stained specimens. We distinguished between osteoid matrix formation and calcification of the bone matrix in the ossification process, but we subsequently referred to as timing of ossification to the onset of calcification to make our observations comparable with most previous works, which reported ossification by recognizing retention of Alizarin Red stain in whole-mounted cleared-and-stained specimens. In addition, we took into account individual variation by means of two different criteria defining the onset of ossification of each bone (Sheil et al., 2014). The onset was determined as the earliest stage at which calcification is apparent: (1) in at least a single specimen (referred hereafter as first-appearance criterion); (2) in 100% of available specimens (referred hereafter as 100% criterion).

The extent of cranial and appendicular ossification during ontogeny was quantified by calculating ossification indexes based on the percentage of elements per skeletal region that were ossified at each particular stage (Supplementary Table S1). For these indexes we computed as one element those bones that are paired (e.g., frontoparietal, femur), serial (e.g., vertebral centra, metatarsals), or form complexes (e.g., radio-ulna, carpals). In view of different approaches observed in the literature to account for individual variation (Dunlap and Sanchiz, 1996; Hanken and Hall, 1984; Sheil et al., 2014), this ossification index was calculated for each stage in three different ways: (1) frequency of element categories (e.g., frontoparietal) that show ossification under the first-appearance criterion (OI1); (2) frequency of element cate-

gories that show ossification under the 100% criterion (OI2); (3) mean frequency of ossification considering all specimens examined independently (OI3). General osteological terminology used in this paper mostly follows that of Trueb (1973) and the taxonomy follows that of Frost (2016). Herein, we focused on the timing and extent of ossification based on different techniques and criteria rather than on the description of anatomical transformations involved during the skeletal development of *R. arenarum*, which will be published elsewhere.

In order to properly contextualize our observations in *R. arenarum* we first compared the timing of ossification of the skull and the appendicular skeleton based on the computed indexes with those of *L. latinasus* (this study) and *Dryophytes chrysoscelis* (Cope, 1880) (Shearman and Maglia, 2015), which are also hyloid anurans with generalized pond-type larvae. Additionally, we gathered from the literature the timing of ossification of bufonid species for which there is comparable data (Badawy et al., 2012; Dunlap and Sanchiz, 1996; Gaudin, 1978; Sedra, 1949; Sedra and Michael, 1958) and of a broad sample of other species (see Supplementary data) to extend our comparisons to the whole anuran clade. Among available ossification sequences, we only considered those that were staged (or could be staged based on published data), relatively complete for at least the skull, and based on the recognition of Alizarin Red stain in cleared-and-stained specimens.

Available data only allowed computing OI1 throughout larval ontogeny for 18 anuran species (Supplementary Table S2). Onset of cranial ossification (first-appearance criterion) could be gathered for nearly a hundred species across Anura, of which we also compiled data on the onset of appendicular ossification (first-appearance criterion) and larval period length for nearly one third of them (Supplementary Table S3). We used this data to compare the relative timing of cranial and appendicular ossification and to test the hypothesis that linked relative delayed cranial ossification with rapid larval development (Dunlap and Sanchiz, 1996). This assumption was tested by comparing the onset of cranial/appendicular ossification ratio based on first-appearance data of species with rapid development (i.e., reported larval period spans less than four weeks) with those with longer larval periods. Additionally, we examined differences in the onset of cranial ossification (first-appearance criterion) relative to Gosner stage among species of different anuran lineages. Significant differences between groupings were tested through Kruskal-Wallis tests, or Welch *F* tests if the Levene test based on medians confirmed unequal variance of the samples ($P < 0.01$). All analyses and graphics were performed in the statistical package PAST 3.0 (Hammer et al., 2001).

3. Results

3.1. Osteogenesis and calcification based on histological serial sections

The first signs of osteogenesis in *R. arenarum* are detected in serial histological sections of prometamorphic tadpoles of GS37, in which the formation of osteoid matrix has already begun in cranial as well as in postcranial elements. This is particularly evident in MMT stained transverse sections at the level of the orbital region of the head and at the anterior part of the vertebral column, in which the osteoid matrix of frontoparietal and neural arch pedicels, respectively, are deeply stained with Aniline Blue (Fig. 1). By this stage, osteocytes surrounded by osteoid matrix are already evident in some of these serial sections (Fig. 1F).

Among cranial elements, those that begin to ossify first are the exoccipitals, frontoparietals, and parasphenoid (Fig. 1A–D). The former are paired chondral bones at the posterior end of the skull that begin to ossify perichondrally at the ventromedial part of the occipital condyles and further extend dorsally along the lateral margins of the foramen magnum during prometamorphosis. The paired frontoparietals and the median parasphenoid are dermal bones that begin to form by intramembranous ossification as a thin layer of osteoid matrix of one to two-cells-thick at GS37–39. Each frontoparietal initially develops at the dorsal edge of the orbital cartilage anterior to the level of the taenia tecti transversalis, extending medially just above a thin layer of dense connective tissue roofing the braincase and above the cranial meninges (Fig. 1A, B). The parasphenoid initially forms adjacent to the cartilaginous chondrocranium immediately anterior to the otic capsules. During prometamorphosis the frontoparietals and parasphenoid extend both anteriorly and posteriorly, although they remain as a thin layer of bone throughout following stages (Fig. 2A, B).

Presacral neural arches and limb bones, which are among the first postcranial elements showing osteoid matrix deposition, begin to ossify perichondrally. As early as GS37, a distinct periosteum and a well-organized osteoid matrix with osteocytes are present in these skeletal elements. The formation of osteoid matrix in the neural arches begins at the level of their pedicels (Fig. 1E, F), but soon extends onto the transverse processes and dorsal laminae. Progressing prometamorphosis ossification in these elements rapidly extends and further proceeds endochondrally, forming peripheral layers of osteoid matrix that are much thicker than those of the dermal cranial bones at the same stage.

Notably, it is not until GS40 that the bone matrix of cranial bones, such as the frontoparietal and parasphenoid (Fig. 2A, B), and neural arches (Fig. 2C, D) begin to calcify, three stages later than the beginning of osteoid matrix formation in these same skeletal elements. This is evidenced by precipitation of silver ions in the von Kossa stained sections, which appears as brownish spots in the calcified bone matrix (Fig. 2D). At GS40 nearly all the already deposited bone matrix of cranial and postcranial elements is homogeneously calcified, and from this stage onwards all new bone matrix that is formed immediately calcifies. This is exemplified by vertebral centra, which, following initial calcification of neural arches, begin to develop bone matrix dorsal to the notochord that also appears calcified at GS41 (Fig. 2E, F). The ossification of the centra then progressively surrounds the notochord ventralwards as a thin sheet of bone.

3.2. Timing and sequence of ossification in Rhinella arenarum based on whole mounts

The examination of cleared-and-stained specimens of *R. arenarum* show that ossification is first detectable at late prometamorphosis on GS40 in different parts of the skeleton based on the first-appearance criterion, but under the 100% criterion ossification does not begin until the onset of metamorphosis (GS42). In general, individual variation in the onset of ossification of particular elements is between one to three stages (Table 1). Ossification of the full complement of bones is not even achieved at the juvenile stage analyzed here, irrespectively of the criterion considered. The timing and sequence of ossification for the cranial, axial, and appendicular skeleton are described below separately. The stage at which different elements begin to ossify is indicated in parentheses both under the first-appearance (first) and 100% criteria (second).

3.2.1. Skull

The first cranial bones to show ossification centers are the paired exoccipitals (GS40/GS42) and frontoparietals (GS40/GS42), closely followed by the ossification of the parasphenoid (GS41/GS43). As has been previously described for other anurans, the frontoparietals begin to ossify above the junctions of the taenia tecti transversalis with the chondrocranial wall, whereas the exoccipitals ossify first at the region of the occipital condyles and the parasphenoid,

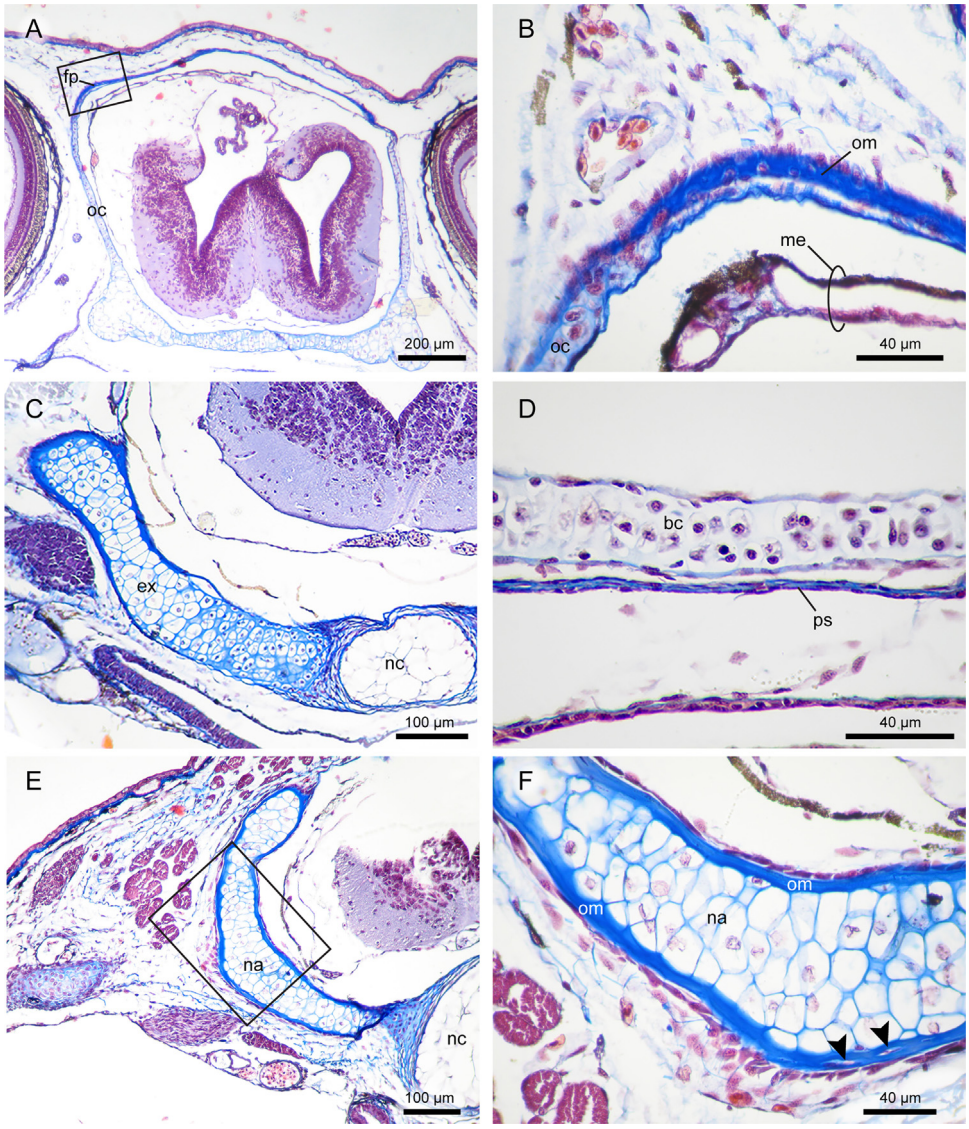

Fig. 1. *Rhinella arenarum*, early signs of osteogenesis in histological transverse sections of prometamorphic tadpoles, MMT stain. (A) General aspect and (B) close-up of frontoparietal, GS37. (C) Exoccipital, GS38. (D) Parasphenoid, GS39. (E) Anterior presacral vertebra and (F) close-up of neural arch, GS37. Abbreviations: bc, braincase; ex, exoccipital; fp, frontoparietal; me, meninges; na, neural arch; nc, notochord; oc, orbital cartilage; om, osteoid matrix; ps, parasphenoid. Black solid arrows depict osteocytes.

as a slit of bone at the anterior level of the solum oticum. These bones are the only ossified cranial elements prior to or shortly after the onset of metamorphosis, depending on the criterion considered, with most other skull bones appearing much later during, or even after, metamorphosis (Table 1). Of the latter, bones of the facial region (premaxilla, maxilla, and septomaxilla) and the lower jaw (dentary and angulosplenial) begin to ossify first (GS44/GS46), closely followed by prootics and nasals (GS44/J). Dermal bones of the suspensorim (squamosals, pterygoids) and mentomeckelian bones start to ossify just around the end of metamorphosis (GS46/J). In the examined stages, each squamosal and pterygoid is restricted to ossification of their ventral and anterior ramus, respectively. Vomers appear after metamorphosis (J), but it is detectable in only one specimen examined. Several cranial bones, including palatines, quadratojugals, sphenethmoid, and columellae, although extensively ossified in the adult toad, are not ossified in any of the larval or juvenile specimens examined.

3.2.2. Vertebral column

Neural arches of the presacral vertebrae (GS40/GS42) are the first elements of the axial skeleton to ossify (Table 1). They appear as paired elements ossified at the level of the bases of the transverse processes, including the lateral part of the neural arch lamina as well as the pedicels. Shortly thereafter, around the onset of metamorphosis (GS41/GS42), the ossification centers of the corresponding vertebral centra, the sacral neural arch, and the neural arches of the coccyx appear. Near the end of metamorphosis, the last axial element to ossify is the hypochord (GS44/GS46).

3.2.3. Girdles and limbs

Elements of the stylopodia and zeugopodia of forelimbs and hindlimbs are among the first bones of the entire skeleton to ossify (GS40/GS42) (Table 1). Ossification begins at their mid-length and slowly spread along the shaft towards the epiphyses. Ilia also ossify relatively early (GS40/GS42) at the level of the proximal region of the ilial shaft. Subsequently (GS41/GS42), scapulae and clavicles of the pectoral girdle, the proximal tarsals (tibiale and fibulare), and the metatarsal IV (just in one specimen) start to ossify first, but shortly after (GS42/GS42) coracoids, cleithra, metacarpals and the remaining metatarsals also show some degree of ossification. Phalanges are among the elements that show more variation in the onset of ossification, yet it is always once metamorphosis has

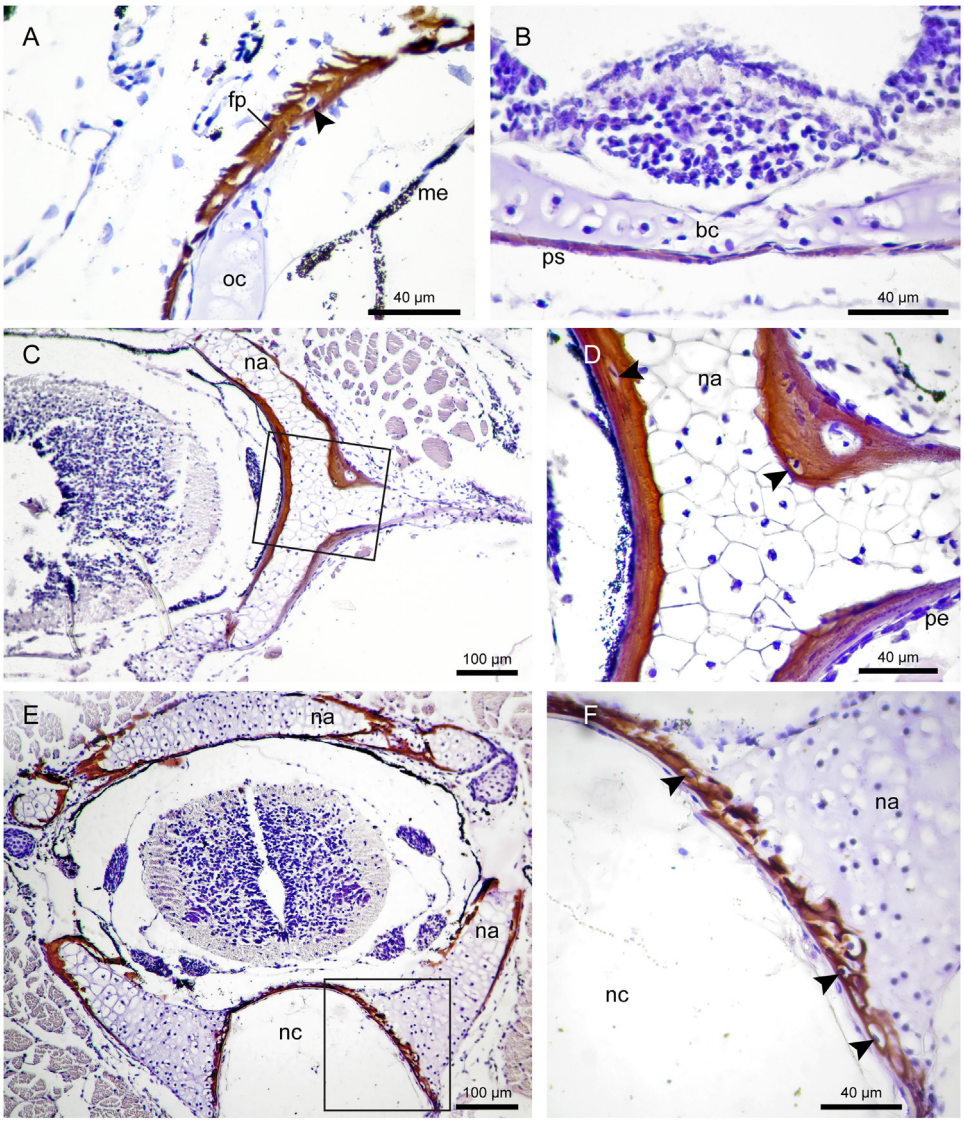

Fig. 2. *Rhinella arenarum*, signs of calcification in histological transverse sections of prometamorphic and metamorphic tadpoles, von Kossa stain. (A) Frontoparietal, GS43. (B) Parasphenoid, GS41. (C) Presacral vertebra and (D) close-up of neural arch, GS40. (E) Presacral vertebra and (F) close-up of contact between neural arch pedicel and centrum, GS41. Abbreviations: bc, braincase; fp, frontoparietal; me, meninges; na, neural arch; nc, notochord; oc, orbital cartilage; ps, parasphenoid; pe, periostium. Black solid arrows depict osteocytes.

already begun, occurring first in the pes (GS42/GS46) and then in the manus (GS44/J). Only some of the examined juveniles (J) show ossification of the ischia, long after these paired elements adjoined to one another. None of the carpal elements shows ossification in any of the specimens examined, yet they are well ossified in the adult toad.

3.3. *Timing and sequence of ossification in* Leptodactylus latinasus

First signs of ossification in *L. latinasus* are evident at late premetamorphosis on GS35 in the exoccipital as well as in the presacral neural arches (Table 2), far earlier than in *R. arenarum* relative to GS (Fig. 3). Shortly thereafter at the very beginning of prometamorphosis (GS36), the exoccipitals, frontoparietals, parasphenoid, and prootics are neatly stained with Alizarin Red in one specimen examined. These cranial elements progressively extend their ossification and are well-ossified in all specimens ending prometamorphosis (GS40-41), although they are the only bones within the skull at that stage. Additional cranial bones appear once metamorphosis has progressed, with nasals, premaxillae, maxillae, and septomaxillae ossifying first (GS44) and bones of the lower jaw, suspensorium, vomers, and quadratojugals ossifying last at the end of metamorphosis (GS46).

Conversely, the postcranial skeleton ossifies faster and more extensively than the skull (Fig. 3; Table 2), with many elements starting to ossify at the beginning of prometamorphosis (GS36/GS37). Among those that ossify first are most limb bones, excluding phalanges and hand bones, scapulae, ilia, and presacral centra. At the end of prometamorphosis (GS41), nearly the full complement of postcranial bones shows at least some degree of ossification in all specimens examined. In the only available newly metamorphosed froglet (GS46) ossification is further evident in the ischia, but the carpal elements remain cartilaginous.

3.4. *Comparative survey of the timing of ossification*

Comparisons between cranial/appendicular onset ossification ratios of species with rapid development with those with longer larval periods (Fig. 4A) allow us to test the assumption that

Table 1
Timing and sequence of ossification in *Rhinella arenarum*.

	Prometamorphosis						Metamorphosis					
Gosner stage	36	37	38	39	40	41	42	43	44	45	46	J
(N)	(6)	(6)	(6)	(6)	(7)	(7)	(7)	(6)	(3)	(3)	(3)	(6)
Exoccipital					1	2						
Frontoparietal					1	1						
Parasphenoid						1	3					
Premaxilla									2	1		
Maxilla									2	1		
Septomaxilla									2	1		
Dentary									2	2		
Angulosplenial									2	2		
Prootic									1	2	1	
Nasal									1	1	1	
Squamosal											1	
Pterygoid											1	
Mentomeckelian											1	
Vomer												1
Palatine												
Quadratojugal												
Sphenethmoid												
Columella												
Humerus					1	3						
Radio-ulna					1	3						
Femur					1	3						
Tibiofibula					1	3						
Ilium					1	3						
Neural arches					1	2						
Centra						1						
Tibiale-Fibulare						3						
Scapula						3						
Clavicle						2						
Metatarsals						1						
Metacarpals												
Coracoid												
Cleithrum												
Phalanges pes							1	0	2	2		
Hypochord									2	0		
Phalanges manus									2	0	1	
Ischium												2
Carpals												

Abbreviations: N, number of specimens; Pre, premetamorphosis. Onset of ossification is indicated in different shades of grey according to the first-appearance criterion (light grey; number of specimens showing ossification is indicated) or the 100% criterion (dark grey).

delayed cranial ossification is linked to rapid larval development in anurans (Dunlap and Sanchiz, 1996). Fast-developing species ($n = 9$) significantly differs from other non-bufonid anurans ($n = 17$) (Kruskal-Wallis test, $H = 9.579$, $P < 0.01$). True toads ($n = 5$) also differ significantly from the latter (Fig. 4A; Kruskal-Wallis test, $H = 5.408$, $P < 0.05$), although the length of their larval periods do not differ from those of most anurans (Supplementary Table S3). Regarding the onset of cranial ossification, based on the first-appearance criterion relative to Gosner stage (Fig. 4B), true toads ($n = 12$) significantly differ from dendrobatids ($n = 5$) (Kruskal-Wallis test, $H = 10$, $P < 0.01$), as well as from other neobatrachians ($n = 69$) (Welch F test, $F = 40.65$, df = 64.35, $P < 0.001$).

4. Discussion

4.1. Osteogenesis and calcification

Exoccipitals, parasphenoid, and frontoparietals ossify first among cranial bones, whereas the sphenethmoid, palatines, and quadratojugals are among those that ossify last (postmetamorphic stages) in *R. arenarum*, a sequence pattern that is largely congruent with that of *L. latinasus*, which is here described in detail for the first time, and most other anurans studied (Hanken and Hall, 1988; Trueb, 1985; Weisbecker and Mitgutsch, 2010).

Most previous work on the timing of ossification in anurans obtained their data from cleared-and-stained specimens, in which a particular bone is considered ossified if it retains Alizarin Red Stain (Shearman and Maglia, 2015; Sheil et al., 2014; and references therein). However, it has been argued that the use of this type of preparations is limited in precisely determining the onset of ossification, since retention of Alizarin Red Stain in this case might reflects proliferation of matrix deposition and calcification rather than early formation of ossification centers (Hanken and Hall, 1988). Comparisons between first-appearance data here obtained from histological serial sections and whole-mounted specimens of *R. arenarum* also support this view, showing that first signs of osteoid matrix deposition in serial sections are evident at least three stages earlier than the respective bones are detectable in cleared-and-stained tadpoles at GS40.

There is also some concern about whether correlation between actual onset of ossification and first detection of Alizarin Red Stain in whole mounts even exists (Sheil et al., 2014). It is worth mentioning, however, that our data show that calcification of cranial and postcranial skeleton in *R. arenarum* is first detectable at stage GS40 by retention of Alizarin Red Stain in whole mounts and equally by precipitation of silver salts on serial sections. Therefore, ossification data gathered from cleared-and-stained specimens, although insufficient to detect early foci of osteoid matrix deposition, might

Table 2
Timing and sequence of ossification in *Leptodactylus latinasus*.

	Pre	Prometamorphosis						Metamorphosis				
Gosner stage	35	36	37	38	39	40	41	42	43	44	45	46
(N)	(2)	(2)	(3)	(2)	(2)	(1)	(3)	(2)	(1)	(1)	(1)	(1)
Exoccipital	1	1										
Frontoparietal		1	2									
Parasphenoid		1	2									
Prootic		1	2	0	1							
Nasal												
Premaxilla												
Maxilla												
Septomaxilla												
Dentary												
Angulosplenial												
Squamosal												
Pterygoid												
Vomer												
Quadratojugal												
Mentomeckelian												
Palatine												
Sphenethmoid												
Columella												
Neural arches	1	1										
Humerus		1										
Radio-ulna		1										
Femur		1										
Tibiofibula		1										
Ilium		1										
Centra		1										
Tibiale-Fibulare		1										
Scapula		1										
Metatarsals		1										
Coracoid		1	2									
Clavicle		1	1									
Cleithrum		1	1									
Phalanges pes		1	1	1								
Metacarpals				1	1							
Hypochord					1							
Phalanges manus					1							
Ischium												
Carpals												

Abbreviations: Nnumber of specimens; Prepremetamorphosis. Onset of ossification is indicated in different shades of grey according to the first-appearance criterion (light grey;number of specimens showing ossification is indicated) or the 100% criterion (dark grey).

reflect accurately the onset of calcification or at least correlates well with it. This finding, if confirmed in other species, is encouraging as it allows assembling all first-appearance ossification data indicating calcification in a single analytical framework.

4.2. Intraspecific variation in the timing of ossification

Individual variation in the timing of ossification has seldom been examined in anurans, although some remarkable examples exist (e.g., de Sá and Swart, 1999; Dunlap and Sanchiz, 1996; Gaudin, 1978; Hanken and Hall, 1984; Shearman and Maglia, 2015; Sheil et al., 2014; Trueb and Hanken, 1992). Here, we found that variation in the timing of ossification relative to GS in *R. arenarum* exists, but is somewhat lower than that reported for other anurans, including bufonids. Variation in the appearance of cranial and most postcranial bones of *R. arenarum*, as evaluated by comparing data derived from first-appearance and 100% criteria, spans up to three GS, phalanges being the only elements that exceed this variation (Table 1). In contrast, maximum variation in the onset of ossification of certain cranial bones ranges from five GS in some distantly related anuran species (*Bombina orientalis* (Boulenger, 1890), *D. chrysoscelis*, *L. latinasus*; Hanken and Hall, 1984; Shearman and Maglia, 2015; Sheil et al., 2014; this study) to eight or nine GS in other bufonids (Dunlap and Sanchiz, 1996; Gaudin, 1978) to as much as 16 GS in some pipids (de Sá and Swart, 1999). This limited variation in the onset of ossification of particular bones in *R. arenarum* might be due to the fact that bones start to ossify later and during a more restricted time frame than in most other anurans (see Section 4.3).

The amount of variation in the timing of ossification could also be assessed for each stage by analyzing variation in the ossification index. In *R. arenarum* this variation is more extensive at late metamorphosis (GS44–46) in the skull, but at late prometamorphosis (GS40–41) in the appendicular skeleton (Fig. 3). A more or less similar pattern is observed in the cranial ossification index of *B. orientalis* (Hanken and Hall, 1984) and in the appendicular data of *Bufo bufo* (Linnaeus, 1758) (Dunlap and Sanchiz, 1996), although direct comparisons between studies are hindered by differences in sampling and coding strategies in the index computation. Therefore, in order to allow meaningful comparisons, we estimated the ossification indexes in these and other anuran species based on published data, but using always the same coding strategy as that used for *R. arenarum* (Supplementary Table S1). These comparisons indicate that there is not a single common pattern of the amount of variation in the ossification index across species (Fig. 3). Even though phylogeny might account for part of the discrepancies, it has been noted that methodological differences regarding fixing and staining protocols, ossification criteria, and animal provenance

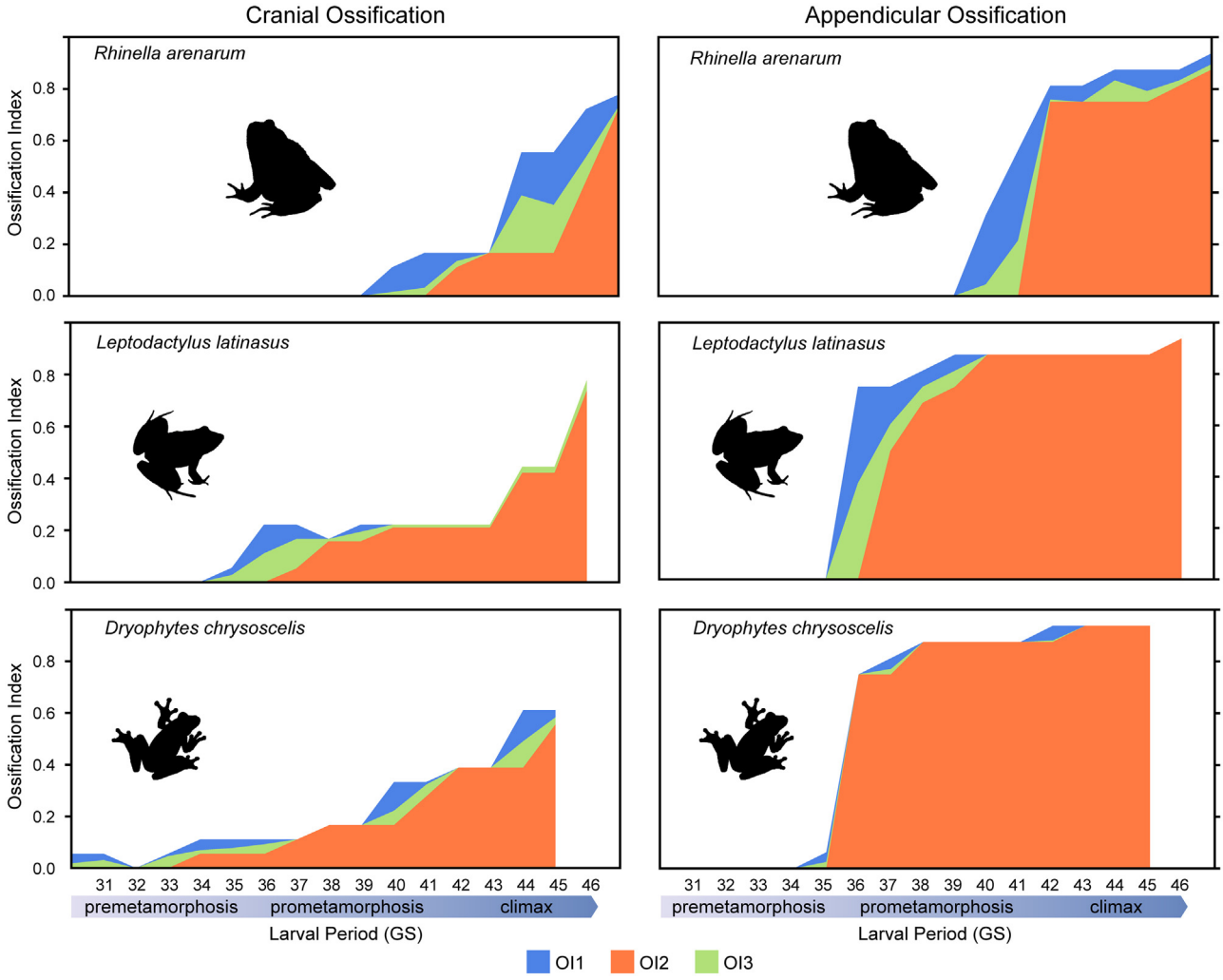

Fig. 3. Ossification indexes according to Gosner stage of the cranial and appendicular skeleton of *Rhinella arenarum*, *Leptodactylus latinasus*, and *Dryophytes chrysoscelis*. Abbreviations: OI1, first-appearance criterion index; OI2, 100% criterion index; OI3, mean frequency index.

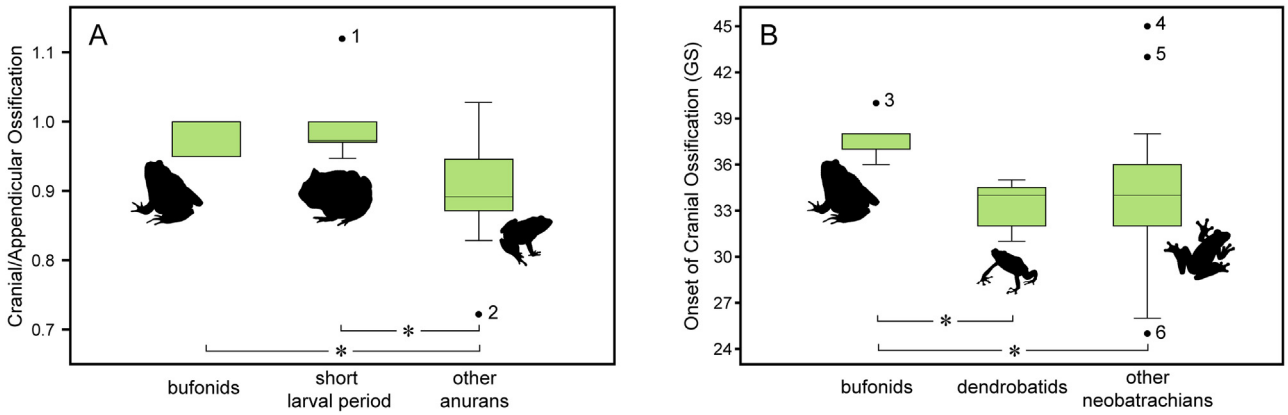

Fig. 4. Box plots showing the onset of cranial ossification based on the first-appearance criterion in bufonids and other anurans relative to (A) the onset of appendicular ossification and (B) Gosner stage. The box plots present medians, 25 and 75 percentiles; limits are the 95% confidence intervals. Outliers are represented as black dots (1, *Dermatonotus muelleri*; 2, *Nasikabatrachus sahyadrensis*; 3, *Rhinella arenarum*; 4, *Osteopilus septentrionalis*; 5, *Eupsophus* spp.; 6, *Ranoidea nannotis*). An asterisk (*) denote significant differences as follows: between non-bufonid species with longer larval periods and fast-developing anurans (Kruskal-Wallis test, $H = 9.579$, $P < 0.01$) and bufonids (Kruskal-Wallis test, $H = 5.408$, $P < 0.05$), respectively; between bufonids and dendrobatids (Kruskal-Wallis test, $H = 10$, $P < 0.01$) and other neobatrachians (Welch F test, $F = 40.65$, df = 64.35, $P < 0.001$), respectively.

(wild-caught versus lab-raised) might also impact on this type of data (e.g., Gaudin, 1978; Shearman and Maglia, 2015; Sheil et al., 2014).

4.3. Timing of cranial and appendicular ossification

In the larvae of *R. arenarum* the cranial and appendicular skeletal regions begin to ossify simultaneously at a late stage (GS40/GS42),

regardless of the ossification criterion considered (Table 1). However, ossification indexes of the appendicular skeleton rises first at a much higher rate than those of the skull (Fig. 3). For instance, by the onset of metamorphosis (GS42) more than 75% of the appendicular bones, but less than 20% of the cranial bones, are ossified. From that point on, ossification of the appendicular skeleton increases only slightly (less than 8%) during larval development, whereas the skull continues to ossify at a more or less constant rate (roughly 9% increase per stage) until the end of metamorphosis (GS46), when scarcely more than half of the cranial bones have already started to ossify (Fig. 3). Even though nearly all anuran larvae for which comparable data is available exhibit a roughly similar pattern of increase of cranial relative to appendicular ossification indexes, in most of them, including those of *L. latinasus* studied herein, the skull starts to ossify prior to the appendicular skeleton and much earlier relative to GS (Fig. 3; Supplementary data).

Similar patterns of delayed cranial relative to appendicular ossification have previously been related to rapid larval development in the true toad *B. bufo* and in the distantly related spadefoot toad *Spea bombifrons* (Cope, 1863) (Dunlap and Sanchiz, 1996). However, the surveyed comparative data regards this explanation unlikely for true toads. It is worth mentioning that this pattern, either in *R. arenarum* or in *B. bufo*, is not linked to a markedly short larval period as in *S. bombifrons* (15–20 days after hatchling; Voss, 1961). The larval period lasts around 45 days in *R. arenarum* (Echeverría and Fiorito De López, 1981), whereas in *B. bufo* has been reported as during a month in lab-raised tadpoles (Semlitsch, 1994) or as much as 62 days in wild-caught embryos maintained in experimental ponds (Brady and Griffiths, 2000), being both within the range of most other anurans (Supplementary Table S3). Additionally, this pattern is similar to that of the few other bufonids for which comparable data is available, including *Epidalea calamita* (Laurenti, 1768) (Dunlap and Sanchiz, 1996) and *Sclerophrys regularis* (Reuss, 1833) (Badawy et al., 2012; Sedra, 1949), which larval periods typically last around 50 days (Brady and Griffiths, 2000; Sedra, 1950). In these true toads the skull begins to ossify at, or nearly at, the same stage as the appendicular skeleton irrespective of the span of the larval period (Fig. 4), thus indicating that this delayed pattern in bufonid toads is not related to fast-developing larvae.

It has to be noted that some anuran species with relatively short larval periods do not show delayed cranial relative to appendicular ossification (Banbury and Maglia, 2006; Haas, 1999), whereas species with relatively long larval periods (more than two months) show a delayed pattern similar to that of bufonids (Davies, 1989; Fabrezi and Goldberg, 2009; Maglia and Pugener, 1998). However, taken as a whole, the surveyed comparative data suggests that some relation might indeed exist between the timing of cranial relative to appendicular ossification and a markedly short larval period (i.e., spanning less than four weeks) in most non-bufonid anuran lineages. In species with rapid development, mainly including South American horned frogs (Ceratophryidae), African bullfrogs (Pyxicephalidae), and North American burrowing toads (Scaphiopodidae) that inhabit arid or semiarid environments, the skull typically starts to ossify, as in bufonids, nearly at the same time as the appendicular skeleton (Fig. 4). Conversely, non-bufonid anurans with larval periods spanning more than a four weeks significantly differ from those with fast-developing larvae and true toads, since ossification in the cranium begins, on average, at least two GS earlier than that of the girdles and limbs (Fig. 4).

4.4. *Delayed ossification in* Rhinella arenarum *and other true toads*

First-appearance data shows that most anurans start to ossify within late premetamorphosis and early prometamorphosis, with only a few species ossifying later than GS38 (Figs. 3, 4), typically the skull ossifying first (GS32–36) followed by the appendicular skeleton (GS35–37). As commented above, first signs of skeletal ossification in cleared-and-stained larvae of *R. arenarum* occur at late prometamorphosis (GS40), noticeably later than in most other anurans. Such a late onset of ossification in this large true toad is striking given the generalized condition of their pond-type larvae and the heavily ossified skeleton of adults (Pérez Ben et al., 2014; Vera Candioti, 2006). The contrast is even greater regarding the skull, which is poorly ossified at the end of metamorphosis, but shows hyperossification of both dermal and chondral bones in the adult toad (e.g., Pérez Ben et al., 2014), indicating a fast rate of ossification during postmetamorphic development.

It is noteworthy that the few other bufonids studied to date also show a somewhat delayed onset of skeletal ossification relative to GS, with most species ossifying later than GS36 (Fig. 4). The combination of a relatively late onset of ossification, according to GS, coupled with the almost concurrent ossification of the cranial and appendicular skeleton observed in true toads is rare among anurans and places them at one end of developmental variation. This late onset of cranial ossification significantly differs from that of the rest of neobatrachians in general and from that of dendrobatids in particular (Fig. 4), which have been recovered recurrently as the sister group of bufonids in recent molecular phylogenetic analyses (e.g., Fouquet et al., 2013; Pyron and Wiens, 2011; Roelants et al., 2007). Unfortunately, ossification data for basal lineages within Bufonidae, such as *Melanophryniscus* Gallardo, 1961; is still lacking. Additional data on the timing of ossification of bufonids is needed to corroborate if the ossification pattern observed in *R. arenarum* and other true toads is synapomorphic at some level within Bufonidae or evolved more than once in this large cosmopolitan clade.

Acknowledgements

This work was supported by Universidad de Buenos Aires [UBACyT 2014–2017 no. 20020130100828BA to G.N.H.]. Scholarship support for E.R. and M.E.A.O. was provided by the Consejo Nacional de Investigaciones Científicas y Técnicas (CONICET). We thank three anonymous reviewers for their helpful comments.

Appendix A. Supplementary data

Supplementary data associated with this article can be found, in the online version, at http://dx.doi.org/10.1016/j.jcz.2017.03.002.

References

Altig, R., Johnston, G.F., 1989. Guilds of anuran larvae: relationships among developmental modes, morphologies, and habitats. Herpetol. Monogr. 3, 81–109.
Attademo, A.M., Sanchez-Hernandez, J.C., Lajmanovich, R.C., Peltzer, P.M., Junges, C., 2017. Effect of diet on carboxylesterase activity of tadpoles (*Rhinella arenarum*) exposed to chlorpyrifos. Ecotox. Environ. Saf. 135, 10–16.
Badawy, G., Sakr, S., Atallah, M., 2012. Comparative study of the skeletogenesis of limb autopods in the developing chick *Gallus domesticus* and toad *Bufo regularis*. RJPBCS 3, 966–988.
Banbury, B., Maglia, A.M., 2006. Skeletal development of the Mexican spadefoot, *Spea multiplicata* (Anura: Pelobatidae). J. Morphol. 139, 439–476.
Boulenger, G.A., 1890. A list of the reptiles and batrachians of Amoorland. Ann. Mag. Nat. Hist. 5 (Ser. 6), 137–144.
Brady, L.D., Griffiths, R.A., 2000. Developmental responses to pond desiccation in tadpoles of the British anuran amphibians (*Bufo bufo*, *B. calamita* and *Rana temporaria*). J. Zool. Lond. 252, 61–69.
Cei, J.M., 1980. Amphibians of Argentina. Monit. Zool. Italiano N.S. Monogr. 2, 1–609.
Cope, E.D., 1863. On *Trachycephalus*, *Scaphiopus* and other Batrachia. Proc. Acad. Nat. Sci. Philadelphia 15, 43–54.
Cope, E.D., 1880. On the zoological position of Texas. Bull. U. S. Natl. Mus. 17, 1–51.
Davies, M., 1989. Ontogeny of bone and the role of heterochrony in the myobatrachine genera *Uperoleia*, *Crinia*, and *Pseudophryne* (Anura: Leptodactylidae: Myobatrachinae). J. Morphol. 200, 269–300.
de Sá, R.O., Swart, C.C., 1999. Development of the suprarostral plate of pipoid frogs. J. Morphol. 240, 143–154.

Dunlap, K.D., Sanchiz, B., 1996. Temporal dissociation between the development of the cranial and appendicular skeletons in *Bufo bufo* (Amphibia: Bufonidae). J. Herpetol. 30, 506–513.
Echeverría, D.D., Fiorito De López, L.E., 1981. Estadios de la metamorfosis en *Bufo arenarum* (Anura). Physis B 40 (98), 15–23.
Etkin, W., 1932. Growth and resorption phenomena in anuran metamorphosis. I. Physiol. Zool. 5, 275–300.
Fabrezi, M., Goldberg, J., 2009. Heterochrony during skeletal development of *Pseudis platensis* (Anura, Hylidae) and the early offset of skeleton development and growth. J. Morphol. 270, 205–220.
Fabrezi, M., 2011. Heterochrony in growth and development in anurans from the Chaco of South America. Evol. Biol. 38, 390–411.
Fouquet, A., Blotto, B.L., Maronna, M.M., Verdade, V.K., Junca, F.A., de Sa, R., Rodrigues, M.T., 2013. Unexpected phylogenetic positions of the genera *Rupirana* and *Crossodactylodes* reveal insights into the biogeography and reproductive evolution of leptodactylid frogs. Mol. Phylogenet. Evol. 67, 445–457.
Frost, D.R., 2016. Amphibian Species of the World: an Online Reference. Version 6.0. American Museum of Natural History, New York, USA (Accessed 18 December 2016). Electronic Database accessible at http://research.amnh.org/herpetology/amphibia/index.html.
Gallardo, J.M., 1961. Nuevo género de Brachycephalidae (Amphibia Anura). Neotropica 7, 71–72.
Garsault, F.A.P.de, 1764. Les Figures des plantes et animaux d'usage en médecine, décrits dans la Matière Médicale de Mr. Geoffroy Médecin. Desprez, Paris.
Gaudin, A.J., 1978. The sequence of cranial ossification in the California toad, *Bufo boreas* (Amphibia, Anura, Bufonidae). J. Herpetol. 12, 309–318.
Gosner, K.L., 1960. A simplified table for staging anuran embryos and ae with notes on identification. Herpetologica 16, 183–190.
Haas, A., 1999. Larval and metamorphic skeletal development in the fast-developing frog *Pyxicephalus adspersus* (Anura, Ranidae). Zoomorphology 119, 23–35.
Hall, J.A., Larsen, J.H., 1998. Postembryonic ontogeny of the spadefoot toad, *Scaphiopus intermontanus* (Anura: Pelobatidae): skeletal morphology. J. Morphol. 238, 179–244.
Hammer, Ø., Harper, D.A.T., Ryan, P.D., 2001. PAST: paleontological statistics software package for education and data analysis. Palaeontol. Electron. 4 (1), 1–9.
Hanken, J., Hall, B.K., 1984. Variation and timing of the cranial ossification sequence of the Oriental Fire-Bellied Toad, *Bombina orientalis* (Amphibia, Discoglossidae). J. Morphol. 182, 245–255.
Hanken, J., Hall, B.K., 1988. Skull development during anuran metamorphosis I. Early development of the first three bones to form—the exoccipital, the parasphenoid, and the frontoparietal. J. Morphol. 195, 247–256.
Harrington, S.M., Harrison, L.B., Sheil, C.A., 2013. Ossification sequence heterochrony among amphibians. Evol. Dev. 15, 344–364.
Hensel, R., 1867. Beiträge zur Kenntnis der Wirbelthiere Südbrasilens. Arch. Naturgesch. 33, 120–162.
Hermida, G.N., Farías, A., 2009. Morphology and histology of the larynx of the common toad *Rhinella arenarum* (Hensel, 1867) (Anura, Bufonidae). Acta Zool. 90, 326–338.
IUCN, 2016. The IUCN Red List of Threatened Species. Version 2016-2. http://www.iucnredlist.org. Downloaded on 04 September 2016.
Jiménez de la Espada, M., 1875. Vertebrados del Viaje al Pacífico Verificado de 1862 a 1865 por una Comisión de Naturalistas Enviada por el Gobierno Español Batracios. Miguel Ginesta, Madrid.
Kiernan, J.A., 1999. Histological and Histochemical Methods, third ed. Hodder Arnold Publications, New York.
Laurenti, J.N., 1768. Specimen Medicum, Exhibens Synopsin Reptilium Emendatum cum Experimentis Circa Venena et Antidota Reptilium Austriacorum, Joan. Thom. Nob. de Trattnern, Wien.
Linnaeus, C., 1758. Systema Naturae per Regna Tria Naturae, Secundum Classes, Ordines, Genera, Species, cum Characteribus, Differentiis, Synonymis, Locis, vol. 1., 10th edition L. Salvii, Stockholm.
Maglia, A.M., Pugener, A., 1998. Skeletal development and adult osteology of *Bombina orientalis* (Anura: Bombinatoridae). Herpetologica 54, 344–363.
Maglia, A.M., 2003. Skeletal development of *Pelobates cultripes* and a comparison of the osteogenesis of pelobatid frogs (Anura: Pelobatidae). Sci. Pap. Mus. Nat. Hist. Univ. Kansas 30, 1–13.
Pérez Ben, C.M., Gómez, R.O., Báez, A.M., 2014. Intraspecific morphological variation and its implication in the taxonomic status of '*Bufo pisanoi*', a Pliocene anuran from eastern Argentina. J. Vert. Paleontol. 34, 767–777.
Pollo, F.E., Bionda, C.L., Salinas, Z.A., Salas, N.E., Martino, A.L., 2015. Common toad *Rhinella arenarum* (Hensel, 1867) and its importance in assessing environmental health: test of micronuclei and nuclear abnormalities in erythrocytes. Environ. Monit. Assess. 187, 1–9.
Pyron, R.A., Wiens, J.J., 2011. A large-scale phylogeny of Amphibia including over 2800 species, and a revised classification of extant frogs salamanders, and caecilians. Mol. Phylogenet. Evol. 61, 543–583.
Regueira, E., Sassone, A.G., Scaia, M.F., Volonteri, M.C., Ceballos, N.R., 2013a. Seasonal changes and regulation of the glucocorticoid receptor in the testis of the toad *Rhinella arenarum*. J. Exp. Zool. Part A 319, 39–52.
Regueira, E., Scaia, M.F., Volonteri, M.C., Ceballos, N.R., 2013b. Anteroposterior variation of the cell types in the interrenal gland of the male toad *Rhinella arenarum* (Amphibia, Anura). J. Morphol. 274, 331–343.
Regueira, E., Dávila, C., Hermida, G.N., 2016. Morphological changes in skin glands during development in *Rhinella arenarum* (Anura: Bufonidae). Anat. Rec. Part A 299, 141–156.
Regueira, E., Dávila, C., Sassone, A.G., O'Donohoe, M.E.A., Hermida, G.N., 2017. Post-metamorphic development of skin glands in a true toad: parotoids versus dorsal skin. J. Morphol., http://dx.doi.org/10.1002/jmor.20661.
Reuss, A., 1833. Zoologischen miscellen. Reptilian. Saurier. Batrachier. Mus. Senckenb. 1, 27–62.
Roelants, K., Gower, D.J., Wilkinson, M., Loader, S.P., Biju, S.D., Guillaume, K., Moriau, L., Bossuyt, F., 2007. Global patterns of diversification in the history of modern amphibians. P. Natl. Acad. Sci. U. S. A. 104, 887–892.
Sedra, S.N., Michael, M.I., 1958. The metamorphosis and growth of the hyobranchial apparatus of the Egyptian toad, *Bufo regularis* Reuss. J. Morphol. 103, 1–30.
Sedra, S.N., 1949. On the Homology of certain elements in the Skull of *Bufo regularis* Reuss (Salientia). Proc. Zool. Soc. Lond. 119, 633–641.
Sedra, S.N., 1950. The metamorphosis of the jaws and their muscles in the toad, *Bufo regularis*, correlated with the changes in the animal's feeding habits. Proc. Zool. Soc. Lond. 120, 405–449.
Semlitsch, R.D., 1994. Evolutionary consequences of nonrandom mating—do large males increase offspring fitness in the anuran *Bufo bufo*? Behav. Ecol. Sociobiol. 34, 19–24.
Shearman, R.M., Maglia, A.M., 2015. Osteological development of cope's gray treefrog, *Hyla chrysoscelis*. Acta Zool. 96, 181–198.
Sheil, C.A., Jorgensen, M., Tulenko, F., Harrington, S., 2014. Variation in timing of ossification affects inferred heterochrony of cranial bones in Lissamphibia. Evol. Dev. 16, 292–305.
Sotelo, M.I., Bingman, V.P., Muzio, R.N., 2015. Goal orientation by geometric and feature cues: spatial learning in the terrestrial toad *Rhinella arenarum*. Anim. Cogn. 18, 315–323.
Trueb, L., Hanken, J., 1992. Skeletal development in *Xenopus laevis* (Anura: Pipidae). J. Morphol. 214, 1–41.
Trueb, L., 1973. Bones, frogs, and evolution. In: Vial, J.L. (Ed.), Evolutionary Biology of the Anurans. University Missouri Press, Columbia, pp. 65–132.
Trueb, L., 1985. A summary of osteocranial development in anurans with notes on the sequence of cranial ossification in *Rhinophrynus dorsalis* (Anura: Pipoidea: Rhinophrynidae). S. Afr. J. Sci. 81, 181–185.
Vaira, M., Akmentins, M., Attademo, M., Baldo, D., Barrasso, D.A., Barrionuevo, S., et al., 2012. Categorización del estado de conservación de los anfibios de la República Argentina. Cuad Herpetol. 26, 131–159.
Vera Candioti, M.F., 2006. Ecomorphological guilds in anuran larvae: an application of geometric morphometric methods. Herpetol. J. 16, 149–162.
Vera, M.C., Ponssa, M.L., 2014. Skeletogenesis in anurans: cranial and postcranial development in metamorphic and postmetamorphic stages of *Leptodactylus bufonius* (Anura: Leptodactylidae). Acta Zool. 95, 44–62.
Voss, W.J., 1961. Rate of larval development and metamorphosis of the spadefoot toad, Scaphiopus bombifrons. Southwest Nat. 6, 168–174.
Wassersug, R.A., 1976. Procedure for differential staining of cartilage and bone in whole formalin fixed vertebrates. Stain Technol. 51, 131–134.
Weisbecker, V., Mitgutsch, C., 2010. A large-scale survey of heterochrony in anuran cranial ossification patterns. J. Zool. Syst. Evol. Res. 48, 332–347.
Wild, E.R., 1997. Description of the adult skeleton and developmental osteology of the hyperossified horned frog, *Ceratophrys cornuta* (Anura: Leptodactylidae). J. Morphol. 232, 169–206.
Yıldırım, E., Kaya, U., 2014. Comparative skeletogenesis of the oriental tree frog *Hyla orientalis* (Anura: Hylidae). Zool. Anz. 253, 361–371.